

Slow relaxation of disordered memristive networks

F. Caravelli,^{1,2} F. L. Traversa,³ and M. Di Ventra³

¹*Invenia Labs, 27 Parkside Place, Parkside, Cambridge CB1 1HQ, UK*

²*London Institute for Mathematical Sciences, 35a South Street, London W1K 2XF, UK*

³*Department of Physics, University of California, San Diego, La Jolla, CA 92093, USA*

Networks with memristive elements (resistors with memory) are being explored for a variety of applications ranging from unconventional computing to models of the brain. Using graph-theoretic tools, we show that the memory dynamics promotes scale-free relaxation even for the simplest model of linear memristors. In this case, we are also able to describe the memory evolution in terms of orthogonal projection operators onto the subspace of fundamental current loops. This orthogonal projection explicitly reveals the coupling between the spatial and temporal sectors of the dynamics and the emergence of a power law relaxation as a superposition of exponential relaxation times with a broad range of scales. This “glassy” behavior suggests a much richer dynamics of memristive networks than previously considered.

The role of memory in the statistical properties of complex networks is emerging as a new direction in this field [1–3]. For instance, it was recently argued that time nonlocality, in and of itself, is enough to generate scale-free networks, without the need of spatial nonlocality [2]. This feature is tantalizingly close to the one employed by swarms (e.g., ants) to solve certain optimization problems [4–7], and is a common feature in physical systems [8].

Within the field of complex networks, the subset of those made of memristors (resistors with memory) is revealing a host of physical properties that are relevant both for their practical use, such as unconventional computing [9–12], as well as to understand the collective behavior and learning abilities of certain biological systems [13–17], including the brain [18, 19]. Again, a key signature of these networks is the presence of time nonlocality; a feature, which coupled with the conservation laws guaranteed by Kirchhoff’s laws, promotes unexpected phenomena, such as first-order phase transitions as a function of memory content [20, 21], avalanches [22], etc.

An important issue, however, that has yet to receive appropriate discussion is the role of memory in the *relaxation to steady state* of memristive networks. In other words, the question “How does an excitation in a disordered network of memristive elements relax to steady state?”, has yet to be answered.

As mentioned above, this is not just an academic exercise: these types of networks are being employed to solve complex problems in a variety of different modes. Hence, an answer to this query bears immediate relevance to the question of how efficient such systems are as computing machines and, ultimately, it may help us understand the operation of the brain.

In this paper, we address precisely this issue, namely we study the role of memory in the relaxation properties of memristive networks. We show that such networks support scale-free temporal correlations. We provide an analytical demonstration of this fact using the simplest model of linear memristors, which are good approximations for a variety of actual physical systems [23–28]. In fact, by means of graph-theoretic tools we show explic-

itly that the spatial and temporal sectors of the dynamics are coupled by orthogonal projections onto the subspace of fundamental current loops. This coupling ensures the emergence of a power law as superposition of exponential relaxations times with a broad range of scales, which is the typical signature of glassy behavior.

The model - Let us then start by considering the exact solution of a linear circuit ¹, written in terms of graph quantities such as the loop matrix description of a circuit [29], focusing on linear memristors. Specifically, we employ a slightly modified version of a widely used linear model of memristors described by the equations that relate the current $I(t)$ to the voltage $V(t)$ [23]:

$$V(t) = R(w, t)I(t) \quad (1)$$

$$\dot{w} = \frac{\mathcal{J}}{\beta} R_{on} I + \alpha w, \quad (2)$$

where w is the internal memory state variable, $\mathcal{J} = \pm 1$ represents the polarity of the memristor, R_{on} the limiting resistance when the memristor is in the conducting phase, and β is a constant. In the case of the memristors of Ref. [23], made of an oxide thin film sandwiched between two metal layers with oxygen vacancies, one has $\beta = \frac{2d^2}{\mu}$, where μ represents the electron mobility and d the size of the memristor. The parameter α quantifies the rate of decay of the memory when all generators are switched off. The memory resistance follows the dynamics

$$\begin{aligned} R(w, t) &= R_{on} (1 - w(t)) + R_{off} w(t) \\ &= R_{on} [1 + (r - 1)w(t)], \end{aligned} \quad (3)$$

with R_{off} the resistance in the insulating phase, and we have defined $r = R_{off}/R_{on}$, typically $r \gg 1$.

For generic linear circuits, it is well known that one can write the solution of the current configuration as a function of the current and voltage sources and the *cycle matrix* A of the graph associated to the circuit [29]. In

¹ At each time t , the equations representing our circuit are linear.

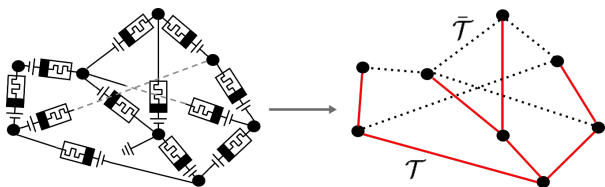


FIG. 1. Small instance of a random memristive network considered in this work with its chord and co-chord decomposition depicted on the right. The formal solutions of the currents can be written in terms of the fundamental loops of the circuit. Given a circuit and an orientation of the currents, we first find a spanning tree \mathcal{T} , which in the figure is given by the red edges. Each element of the tree, \mathcal{T} is a *chord*. Every remaining edge which is not in the spanning tree set is called *co-chord*; for each *co-chord* it is possible to assign a *mesh* variable or *fundamental loop*.

order to understand the derivation in simple terms, consider Fig. 1. The cycle matrix is a rectangular matrix of size $L \times M$, where L is the number of *fundamental loops* and M the number of resistors/memristors. Its introduction is motivated by the following observation: due to the Kirchhoff's constraints on the currents, only a certain number of currents – which equals the number of fundamental loops of the circuit – are linearly independent. The number of fundamental loops can be easily calculated from basic graph theory [30], $L = M - N + 1$, where N is the number of nodes of the circuit, and $N - 1$ is the number of edges in the tree \mathcal{T} , called chords. The complementary set of edges is denoted with $\bar{\mathcal{T}}$, and these edges called co-chords. Therefore, the number of fundamental loops is equal to the number of co-chords.

To be specific, let us consider the case in which there are no current sources, only voltage sources parametrized as elements of a vector $\vec{S}(t)$ on the set of edges (or arcs) of the graph. Similarly, let us introduce a diagonal matrix of (mem)ristances $R = \text{diag}(R_i)$, where the index i runs over the edges of the network. The formal solution of the current configuration, \vec{i} , as a function of R , \vec{S} and A is then given by [29]:

$$\vec{i} = -A^t (ARA^t)^{-1} A\vec{S}(t). \quad (4)$$

The derivation is standard but elegant and is provided for completeness in the Supplemental Material. Equation (4) is the starting point of our analysis. We consider the physically relevant case of a decay to the R_{off} state when there are no sources in the circuit. This is consistent with experimental observations (see, e.g., [12]). Given a diagonal matrix P such that $P = \text{diag}(\sigma_1, \dots, \sigma_M)$, where σ_j is 1 for all memristors up to M , one has $\bar{R} = PR$, where R is still a positive diagonal matrix and contains the absolute values of the resistances. We can however absorb the matrix P into the matrix A , by defining $\bar{A} = AP$.

We now note that the resistance matrix is the one of linear memristors as in Eq. (3), where we introduce the

internal memory vector $\vec{W} = \{w_i\}$, i.e.,

$$R = \text{diag}(R_{on}(\vec{1} + (r-1)\vec{W}(t))). \quad (5)$$

If we introduce the diagonal matrix $W = \text{diag}(\vec{W})$, we can then write the equation for the internal memory states as the following equation

$$\begin{aligned} \frac{d\vec{W}}{dt} &= \alpha\vec{W} \\ &- \frac{1}{\beta} \mathcal{J} A^t (\bar{A}A^t + (r-1)\bar{A}W A^t)^{-1} A\vec{S}(t), \end{aligned} \quad (6)$$

where \mathcal{J} is the matrix which contains the polarity of the memristors. For $\alpha > 0$ the resistance decays to the R_{off} state in the absence of sources, and for $\alpha < 0$ to the R_{on} state. This term is independent from the cycle matrix A , meaning that this is a property of each single memristor, and not a global network effect. We consider the case of homogeneous memristor properties, i.e., they all have identical off and on states. It is of course easy to generalize our results to the inhomogeneous case.

These equations are insofar general. For any circuit, the inverse of $\bar{A}A^t + (r-1)\bar{A}W A^t$ exists so long as R has all non-zero entries on the diagonal, which is the case if both R_{on} and R_{off} are either positive or negative. In order to simplify the notation, we introduce the matrix $\bar{\Omega} = A^t(\bar{A}A^t)^{-1}\bar{A}$, and $\bar{S} = P\vec{S}$. By construction, $\bar{\Omega}$ is an orthogonal projector onto the subspace of fundamental current loops if all resistances in the circuit are all either positive or negative, while it is non-orthogonal there is a mixture of positive and negative resistances.

Let us now set $\xi = r - 1$. After a lengthy but trivial computation we then derive the following equation for the internal memory (see Supplemental Material):

$$\frac{d\vec{W}}{dt} = \alpha\vec{W} - \frac{1}{\beta} \mathcal{J} (\hat{I} + \xi \bar{\Omega}W)^{-1} \bar{\Omega}\bar{S}(t), \quad (7)$$

with \hat{I} the identity matrix. This is the central result of our paper. It is a compact equation that describes the dynamics of the internal memory states of memristors in linear circuits based upon projection operators.

Few comments are in order. First of all, eq. (7) has been derived with the assumption of invertibility of W . Strictly speaking, this means that we are considering the bulk of the dynamics, i.e., when no memristor is in the R_{on} state. Nevertheless, the final formula is independent of W^{-1} and is numerically well-behaved for $w_i \approx 0$, which suggests it can be extended to the boundaries as well.

In addition, Eq. (7) satisfies all the network constraints and Kirchhoff's laws. The importance of the number of fundamental loops is shown by the fact that $\dim(\text{Span}(\bar{\Omega})) = M - N + 1 \equiv L$, which implies that the operator $\bar{\Omega}$ contains information only on the fundamental loops of the circuit.

We have that $P \rightarrow \hat{I}$, and thus $\bar{\Omega} \rightarrow \Omega$, where $\Omega = A^t(AA^t)^{-1}A$ is an orthogonal projection. This implies that we can always decompose any matrix or vector $R = \Omega R + (\hat{I} - \Omega)R = R_\Omega + \bar{R}$, with $\Omega R = R_\Omega$. For the case of passive components, we can identify the operator $\Gamma = (I - \Omega)$ as $B(B^tB)^{-1}B^t$, with B being the reduced incidence matrix (see Supplemental Material).

Given the matrix $(A \ B^t)$, we can write the identity $I = (A \ B^t)(A \ B^t)^{-1}$ and using the fact that $B^tA = 0$, it is easy to prove that $I = A^t(AA^t)^{-1}A + B(B^tB)^{-1}B^t = \Omega + \Gamma$, which provides a nice interpretation for the complementary projector. Moreover, the separation between linearity and non-linearity is explicit in eqn. (7) and is controlled by the constant $r - 1 = (R_{off} - R_{on})/R_{on}$.

We now study the consequences of equation (7) numerically focusing on passive elements only. We take advantage of the fact that there is a simple parametrization for projector operators, given that we are interested in the *average* properties of the dynamics. In this way, the only two relevant parameters are M and N , the number of memristors and the number of nodes, respectively. We then generate a random matrix A of size $L \times M$ and evaluate the matrix Ω according to the equation $\Omega = A^t(AA^t)^{-1}A$. The matrix A is of the form $A = (I \ A_\tau)$, where A_τ is generated using random entries with probability $1/3$ for the discrete values $\{-1, 0, 1\}$. We then consider the quenched dynamics for the memory parameters w_i by integrating eq. (7) numerically using an explicit Euler method and studying the relaxation to steady state. In addition to the bulk equation, we also included the constraints on the internal memory states $0 < w_i < 1$.

For the present paper we focus on the case without active components, i.e., we set $P = \hat{I}$. We provide the evolution of the average memory parameters $\langle w \rangle$ as a function of time for each single realization in Fig. 2 (top). The important physical parameter is r .

Large-memory limit - We consider first the limit $r \gg 1$ and choose in the numerics $r \approx 1000$. The blue and red curves represent the average parameters for the superior and inferior boundary of the memory, respectively. In Fig. 2 (bottom) we plot the best fit with power law (red curve) $\langle w(t) \rangle \approx t^{-\rho}$, with $\rho \approx 0.93$, where the top boundary has been inverted, i.e., $\langle w \rangle' = 1 - \langle w \rangle$. (Finite size effects are discussed in the Supplementary Material.)

Let us approximate the curve of each memristor as an exponential, $w_i(t) = w_i^0 e^{-\lambda_i t}$, where w_i^0 is the initial value of the i th memristor. We focus only on the memristors which converge to $w_i = 0$ values. We then assume that there exists a certain distribution $P(\lambda)$ of decay times, λ_i .

The average behavior of the internal memory is thus given by:

$$\langle w_i(t) \rangle \approx \langle w_i^0 \rangle \int e^{-\lambda t} P(\lambda) d\lambda \quad (8)$$

where we assumed that w_i^0 and λ_i are uncorrelated. If we introduce the inverse time scale $\tilde{\lambda}$, $P(\lambda) = \tilde{\lambda} e^{-\frac{\lambda}{\tilde{\lambda}}}$, one

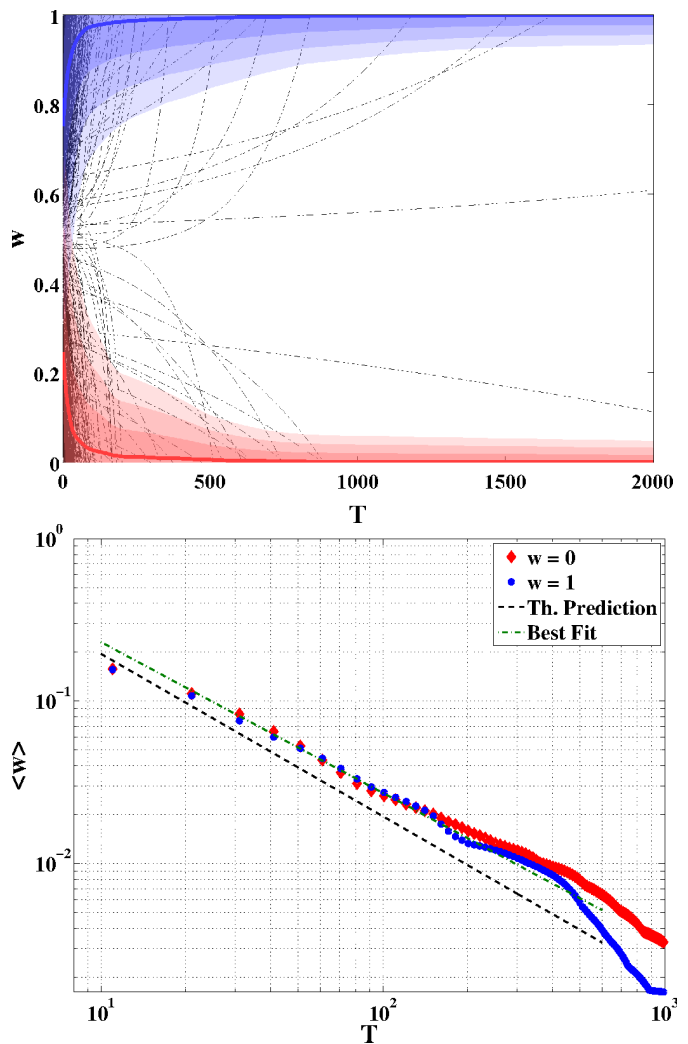


FIG. 2. Average thermalization of the internal memristor memory as a function of time, made assuming that $M = 600$, $L = 300$ for input voltages chosen at random in $[-5, 5]$ Volts and $\beta = 10^{-1}$. *Top*: Simulation of eqn. (7) for a single instance of the randomly selected projector for each memristor (black dashed curves) and their means for those approaching $w = 1$ limit (blue curve) and $w_i = 0$ (red curve). The shading represents the error at 1, 2 and 3 σ to show the sensitivity of the relaxation. *Bottom*: Best fits in the power law regime of the average memory parameters as a function of time for the $w_i = 0$ (blue) limit and $w_i = 1$ (in red, where we plot $1 - \langle w \rangle$) and the best fit (black dashed curve). We observe a relaxation behavior which is compatible with a power law $\langle w(t) \rangle \approx t^{-\rho}$, with a best fit exponent of $\rho \approx 0.93$, against the $\rho = 1$ predicted theoretically.

has

$$\langle w_i(t) \rangle = \frac{\tilde{\lambda}}{2} \int_0^\infty e^{-\frac{\lambda}{\tilde{\lambda}}} e^{-\lambda t} d\lambda = \frac{1}{2} \frac{1}{1 + \tilde{\lambda} t} \quad (9)$$

where $\tilde{\lambda}$ is an artificial time scale, playing the role of a cutoff. We thus obtain the result that for $t \gg \frac{1}{\tilde{\lambda}}$, on average, memristors thermalize to the steady state as $\approx 1/t$.

Low-memory limit - In order to understand the relation between the spectrum of time-scales, the matrix Ω and the sources \vec{S} , we now consider the dynamics in the opposite limit, namely $r \approx 1 \rightarrow \xi \ll 1$. In this case, we approximate the inverse $(\hat{I} + \xi \bar{\Omega} W)^{-1}$ with $\approx \hat{I} - \xi \bar{\Omega} W$. We can thus write:

$$\begin{aligned} \frac{dw_i}{dt} &\approx \alpha w_i - \frac{1}{\beta} ((I - \xi \bar{\Omega} W) \bar{\Omega} \vec{S})_i \\ &= \alpha w_i - \frac{\xi}{\beta} \sum_{jkt} \bar{\Omega}_{ij} w_j \delta_{jk} \bar{\Omega}_{kt} \bar{S}_t + s_i \\ &= \sum_j \left(\alpha \delta_{ij} - \frac{\xi}{\beta} \sum_t \bar{\Omega}_{ij} \bar{\Omega}_{jt} \bar{S}_t \right) w_j + s_i \\ &\equiv \sum_j O_{ij} w_j + s_i, \end{aligned} \quad (10)$$

where $s_i = \frac{\xi}{\beta} \sum_j \bar{\Omega}_{ij} \bar{S}_j$. The solution of this equation is given by:

$$\vec{w}(t) = e^{Ot} \left(\vec{w}^0 + \int_{t_0}^t e^{-O\tilde{t}} \vec{s}(\tilde{t}) d\tilde{t} \right). \quad (11)$$

In the case of a dc-controlled memristive network, e.g. $\vec{s}(t) = \vec{s}$, inevitably the memristors will reach their boundary values 1 or 0. If we, however, focus on the short dynamics of memristors, it is interesting to study the distribution of eigenvalues of the matrix O . For the case of random matrices O with passive components, the distribution of eigenvalues is given in Fig. 3. The first observation is that the distribution is symmetrical and that for $L/M \rightarrow 1$ the distribution flattens out. Given that we have randomly generated voltages on the memristors in $[V/2, V/2]$ with $V = 100$, we observe that in this limit λ of eqn. (9) can be roughly assumed to be $V/2$.

The emergence of a scale-free thermalization of the mean internal parameter shows that disordered memristive networks exhibit an *aging* phenomenon, typical of glassy materials [31, 32]. Although being dramatically different, an analogy to the Sherrington-Kirkpatrick model stems naturally in our analysis: the circuit graph generated at random induces a random projector Ω , which in turn induces a random coupling matrix $(I + \xi \Omega)^{-1}$. Therefore, in this simple model there is no notion of distance, and thus there is strong non-locality. We cannot thus discuss of spatial correlations which fall off as a power law. The case of circuits in which it is possible to define a Hamming distance between memristors will be studied elsewhere [33].

Conclusions - In conclusion, we have derived a matrix differential equation for the evolution of the internal memory states of linear current-driven memristors in a circuit. The differential equation is general and solves the circuit constraints based upon the graph theoretic

cal derivation of the current configuration, using the formalism of spanning trees and fundamental loops in networks. Such equation establishes a very clear connection

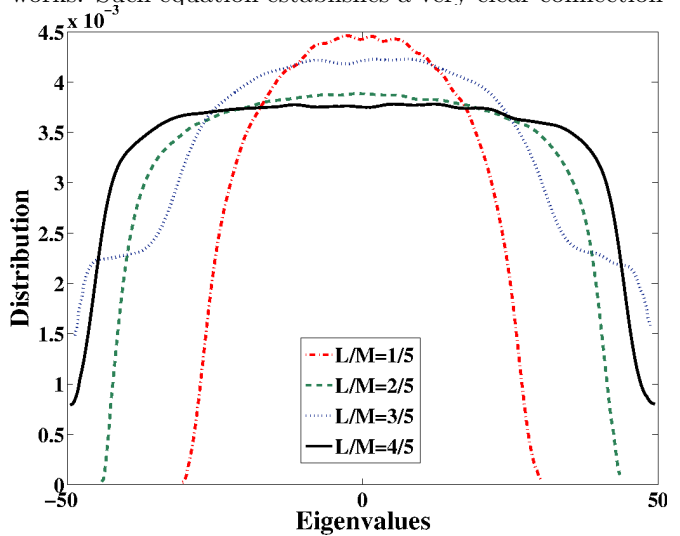


FIG. 3. Distribution of eigenvalues of the matrix O [Eq. 10] for the case of random loop matrices A and $S = [-50, 50]$ randomly generated, and averaged over 500 iterations, where the zero eigenvalues have been removed. We plot $L/M = 1/5, 2/5, 3/5$ and $4/5$ with $M = 500$. The distributions have been smoothed using gaussian kernels, and are zero outside the specified range.

between the theory of projector operators and the dynamics of linear circuits. In particular, we have found that the network dynamics of the internal memory of the circuit can be constructed from only a single matrix, the projector on the space of fundamental loops of the circuit, which contains the information on the network topology and the conservation laws. This shows that the internal memory of the memristors is insensitive to certain forcing modes which fall in the kernel of the projection operator.

Using such equation as a tool and focusing on the case of dc-controlled circuits, we have provided sufficient evidence that the average relaxation of the internal memory to the boundary values is far from exponential. We have shown this by generating random projection operators, but such result is consistent with simulations performed using memristive random circuits. We have also given arguments that the slow relaxation is due to the superposition of memristors decaying with a broad range of time scales at least in the regime of “shallow” memory, i.e., when non-linearities are negligible. These results reveal the rich dynamics of complex networks with memory and establishes a new research direction in memristive circuits.

Two of us (FLT and MD) acknowledge partial support from the Center for Memory Recording Research at UCSD. FC thanks Invenia Labs for support.

-
- [1] C. L. Vestergaard, M. Genouis, A. Barrat, How memory generates heterogeneous dynamics in temporal networks, *Phys. Rev. E* 90, 042805 (2014)
- [2] F. Caravelli, A. Hamma, M. Di Ventra, Scale-free networks as an epiphenomenon of memory, *EPL*, 109, 2 (2015)
- [3] F. Caravelli, Trajectories entropy in dynamical graphs with memory, *Front. Robot. AI* 3, 18 (2016), arXiv:1511.07135
- [4] M. Dorigo, L. M. Gambardella, Ant colonies for the traveling salesman problem, *Biosystems* 43, 2, p 73-81 (1997)
- [5] F. L. Traversa and M. Di Ventra. Universal memcomputing machines. *IEEE Trans. Neural Netw. Learn. Syst.*, (DOI: 10.1109/TNNLS.2015.2391182, preprint arXiv:1405.0931) (2015)
- [6] F. L. Traversa, C. Ramella, F. Bonani, M. Di Ventra, Memcomputing NP-complete problems in polynomial time using polynomial resources and collective states, *Science Advances*, Vol. 1, no. 6, pag e1500031 (2015)
- [7] F. L. Traversa, M. Di Ventra, Polynomial-time solution of prime factorization and NP-hard problems with digital memcomputing machines, arXiv:1512.05064
- [8] Y. V. Pershin and M. Di Ventra. Memory effects in complex materials and nanoscale systems. *Advances in Physics*, 60:145–227 (2011)
- [9] G. Indiveri, S.-C. Liu, Memory and information processing in neuromorphic systems, *Proceedings of IEEE*, 103:(8) 1379-1397 (2015)
- [10] F. L. Traversa, Y. V. Pershin, and M. Di Ventra. Memory models of adaptive behaviour. *IEEE Trans. Neural Netw. Learn. Syst.*, 24:1437 – 1448, 2013.
- [11] Avizienis AV, et al., Neuromorphic Atomic Switch Networks. *PLoS ONE* 7(8): e42772. (2012)
- [12] A. Z. Stieg, Avizienis, et al., Emergent Criticality in Complex Turing B-Type Atomic Switch Networks. *Adv. Mater.*, 24: 286-293 (2012)
- [13] M. Di Ventra and Y. V. Pershin. The parallel approach. *Nature Physics*, 9:200 (2013)
- [14] Y. V. Pershin and M. Di Ventra. Solving mazes with memristors: a massively-parallel approach. *Phys. Rev. E*, 84:046703 (2011)
- [15] A. Adamatzky, G. Chen, Chaos, CNN, Memristors and Beyond, World Scientific (2013)
- [16] Y. V. Pershin and M. Di Ventra. Self-organization and solution of shortest-path optimization problems with memristive networks. *Phys. Rev. E*, 88:013305 (2013)
- [17] Y. V. Pershin, S. La Fontaine, and M. Di Ventra. Memristive model of amoeba learning. *Phys. Rev. E*, 80:021926, 2009.
- [18] D. R. Chialvo, Emergent complex neural dynamics *Nature Physics* 6, 744-750 (2010)
- [19] Y. V. Pershin and M. Di Ventra. Experimental demonstration of associative memory with memristive neural networks. *Neural Networks*, 23:881 (2010)
- [20] T. Driscoli et al., Phase-transition driven memristive system, *App. Phys. Lett.* 95, 043503 (2009)
- [21] Y. V. Pershin, V. A. Slipko, M. Di Ventra, Complex dynamics and scale invariance of one-dimensional memristive networks, *Phys. Rev. E* 87, 022116 (2013)
- [22] F. C. Sheldon, M. Di Ventra, First-Order Phase Transitions in Memristive Networks, arXiv:1601.05772
- [23] D.B. Strukov, G. Snider, D.R. Stewart, and R.S. Williams, “The missing memristor found”, *Nature* 453, pp. 80-83 (2008)
- [24] DB Strukov and KK Likharev. CMOL FPGA: a reconfigurable architecture for hybrid digital circuits with two-terminal nanodevices. *Nanotechn.*, 16:888–900 (2005).
- [25] L. O. Chua and S. M. Kang. Memristive devices and systems. *Proc. IEEE*, 64:209–223, 1976.
- [26] M. Di Ventra, Y. V. Pershin, and L. O. Chua. Circuit elements with memory: Memristors, memcapacitors, and meminductors. *Proc. IEEE*, 97(10):1717–1724 (2009)
- [27] J. J. Yang, D. B. Strukov, D. R. Stewart, Memristive devices for computing, *Nature Nanotechnology* 8 (2013)
- [28] V.A. Demina, et al., Hardware elementary perceptron based on polyaniline memristive devices, *Organic Electronics* 25, 16-20 (2015)
- [29] J. W. Nilsson, *Electric Circuit*, Addison-Wesley (1993)
- [30] B. Bollobas, *Modern Graph Theory*, Springer Science, New York (1998)
- [31] D. Sherrington, S. Kirkpatrick, Solvable model of a spin-glass, *Phys. Rev. Lett.* (26): 1792-1796 (1975)
- [32] E. Vincent, Aging, rejuvenation and memory: the example of spin glasses, *Lect. Notes in Phys.* 716, 7-60 (2007)
- [33] F. Caravelli, F. L. Traversa, M. Di Ventra, in preparation.

Supplementary Material

Appendix A: Formal solution of linear circuits

In this section we recall the basics of graph theory used to derive Eq. (B4) and provide the notation used throughout the main text [29, 30]. We start by considering a graph G with N nodes and M edges which describes the topology of a resistive circuit. As it is standard practice, we then introduce an orientation \mathcal{O} for the currents circulating on the graph, which has 2^m possible configurations, with m being the number of edges (or arcs). From the point of view of graph theory, the graph representing the circuit must be connected, and the degree of each node i satisfies $d_i > 2$. For each node, we can introduce a potential vector p_α , and for each edge a current i_k , where we use latin indices for the edges, and greek indices for the nodes; greek indices with tildes represent instead cycles on the graph. Given an orientation \mathcal{O} , we can introduce two matrices: $B_{\alpha k}^{\mathcal{O}}$, which is a matrix of size $N \times M$, and a cycle matrix $A_{\xi m}^{\mathcal{O}}$, which is of size $C \times M$, where C is the number of cycles of the graph. From now on, we will suppress the orientation apex for simplicity. A valid current configuration is one in which $\sum_{j=1}^M B_{\alpha j} i_j = B\vec{i} = 0$, which represents the Kirchhoff Current Law (KCL). In order for B to have the linear independence of the rows, one row has to be removed, introducing thus the *reduced incidence matrix*. In the following, we will thus consider only results derived with this matrix rather than the full one.

Given a potential vector based on the nodes, the vector of voltages applied to each edge can be written as $\{\bar{v}\}_k = v_k = \sum_{\xi} B_{\xi k}^t p_\xi$, where t represents the matrix transpose. The Kirchhoff Voltage Law (KVL) can thus be written as $\sum_k A_{\xi k} v_k = 0$, an equation which is simply saying in graph theory terms that the circulation of the voltage on edges belonging to a cycle (or *mesh* in circuits) must be zero. This automatically implies that in general $B \cdot A^t = A \cdot B^t \equiv 0$. Analogously, this implies that $\vec{i} \cdot \vec{v} = 0$, which represents the conservation of energy, or *Tellegen's theorem* in circuits.

Let us now introduce a spanning tree \mathcal{T} (*co-chords*), and the set of edges of the graph not included in the tree as $\bar{\mathcal{T}}$, or *chords*, are given by $\bar{\mathcal{T}}$. For each element of the chord $\bar{\mathcal{T}}$, we assign a cycle, called *fundamental loop*. The number of fundamental loops is given by $L = M - N + 1$. As a matter of fact, each current can be written as a superposition of the currents flowing in the fundamental loops, denoted with $j_{\bar{\xi}}$, and one has that $\vec{i} = A^t \vec{i}_c$. In the basis in which we reorder the edges in the tree to come first, one can write $A = (A_{\mathcal{T}}, A_c)$, and since now A_c corresponds to fundamental cycles, A_c is the identity matrix, $A_c = I$. A similar rearrangement can be made also for the incidence matrix B , and thus one has $(B_{\mathcal{T}}, B_c) \cdot (A_{\mathcal{T}}, I)^t = 0$, which implies $A_{\mathcal{T}}^t = -B_{\mathcal{T}}^{-1} B_c$. We now note that since $B\vec{i} = 0$, one has $B_{\mathcal{T}} \vec{i}_{\mathcal{T}} + B_c \vec{i}_c =$

$0 \rightarrow \vec{i}_{\mathcal{T}} = -B_{\mathcal{T}}^{-1} B_c \vec{i}_c = A_{\mathcal{T}}^t \vec{i}_c$. Since $A_c = I$, this implies that $\vec{i} = (A_{\mathcal{T}}^t \vec{i}_c, \vec{i}_c) = A^t \vec{i}_c$. Since A is derived from the *reduced incidence matrix*, this is called *reduced loop matrix*.

If we now write the equation for the circuit, i.e., $\vec{v} = R\vec{i} + \vec{S}(t)$, we note that applying the operator A on the left, we obtain the identity $A\vec{v} = 0 = AR\vec{i} + A\vec{S}(t)$. We now use $\vec{i} = A^t \vec{i}_c$, and obtain $(ARA^t) \vec{i}_c = -A\vec{S}_0(t)$. If we now write the solution of the current, we obtain

$$\vec{i} = A^t \vec{i}_c = -A^t (ARA^t)^{-1} A\vec{S}(t). \quad (\text{A1})$$

which is the starting point of this paper. We stress that since A is derived from a reduced incidence matrix, then ARA^t is always invertible for non-zero resistances.

Appendix B: Derivation of the main dynamical equation

The starting point of the derivation is Eq. (A1). We consider the convention in which $w = 0$ corresponds to R_{on} and $w = 1$ to R_{off} , which is a memristor with opposite polarity to the one introduced in [23]. First of all, let us first say that it is easy to parametrize the presence of active components. In this case, one can simply introduce negative resistances in Eq. (A1), for instance introducing a matrix $P = \text{diag}(\pm 1, \dots, \pm 1)$, where $+1$ are assigned to passive components, while -1 to active components. It is easy to see that P satisfies the property $P^2 = I$. The resistances are thus encoded in the matrix $\tilde{R} = PR = RP$, and Eq. (A1) simply becomes

$$\begin{aligned} \vec{i} &= -A^t \left(A\tilde{R}A^t \right)^{-1} A\vec{S}(t) \\ &= -A^t \left(APRA^t \right)^{-1} A\vec{S}(t) \\ &= -A^t \left(\bar{A}RA^t \right)^{-1} A\vec{S}(t). \end{aligned}$$

As in the main text, we define the matrix $\bar{A} = AP$ and we also use the dynamical properties of the memristors, $\frac{d}{dt} w_j = \mathcal{J}_j(R_{on}/\beta) i_j + \alpha w_j$, with \mathcal{J}_j representing the polarity of the memristor. The goal of this section is to derive a dynamical equation which is in terms of projectors only. For this purpose, we use the Woodbury identity to write the equation in terms of projector only,

$$(Q + UCV)^{-1} = Q^{-1} (I - U(C^{-1} + VQ^{-1}U)^{-1} VQ^{-1}) \quad (\text{B1})$$

where Q and C are square matrices of size n and k respectively, and V and U are rectangular matrices, and which is valid as long as Q and C have inverses.

We first introduce the parameter $\xi = r - 1$ which, as it will become clear soon, can be thought of as the amount of nonlinearity present in the system. Using Eq. (B1), we are thus able to rewrite the inverse $(\bar{A}RA^t)^{-1}$, obtaining:

$$(\bar{A}A^t + \xi \bar{A}W A^t)^{-1} = (\bar{A}A^t)^{-1} \left(I - \bar{A} \left(\frac{W^{-1}}{\xi} + \bar{\Omega} \right)^{-1} A^t (\bar{A}A^t)^{-1} \right) \quad (\text{B2})$$

where we introduced the operator $\bar{\Omega} \equiv A^t (\bar{A}A^t)^{-1} \bar{A}$. It is important to say that the operator $\bar{A}A$ is invertible, as we are considering the reduced loop matrix, and \mathcal{J} is

$$\frac{\beta}{R_{on}} \frac{d\vec{W}}{dt} = -\frac{1}{R_{on}} \mathcal{J} A^t (\bar{A}A^t)^{-1} \bar{A} (I - \xi W) A^t (\bar{A}A^t)^{-1} A S(\tilde{t}) + \frac{\beta\alpha}{R_{on}\beta} \vec{W} + \frac{\xi^2}{R_{on}} \mathcal{J} \bar{\Omega} (I + \xi W \bar{\Omega})^{-1} W \bar{\Omega} W A^t (\bar{A}A^t)^{-1} A \vec{S},$$

where we introduced $\mathcal{J} = \text{diag}(\mathcal{J}_i)$. If we now use the identity $P^2 = I$, we can write $\vec{S} = P^2 \vec{S} = P \bar{S}$, and obtain the equation

$$\begin{aligned} \frac{\beta}{R_{on}} \frac{d\vec{W}}{dt} = & -\frac{\mathcal{J}}{R_{on}} \bar{\Omega} (I - \xi W) \bar{\Omega} \bar{S}(t) + \frac{\beta\alpha}{R_{on}} \vec{W} \\ & + \frac{\xi^2}{R_{on}} \mathcal{J} \bar{\Omega} (I + \xi W \bar{\Omega})^{-1} W \bar{\Omega} W \bar{\Omega} \bar{S}(t), \end{aligned} \quad (\text{B3})$$

in which we used the fact that $[W, \bar{S}] = 0$ since the two matrices are diagonal and $\mathcal{J} = I$. Finally, we use the fact that $\bar{\Omega} (I + \xi W \bar{\Omega})^{-1} = \bar{\Omega} \sum_{k=0}^{\infty} (-\xi W \bar{\Omega})^k = \sum_{k=0}^{\infty} (-\xi \bar{\Omega} W)^k \bar{\Omega} = (I + \xi \bar{\Omega} W)^{-1} \bar{\Omega}$, and obtain the final result shown in Eq. (B4). Using the matrix Taylor expansion in $\xi = r - 1$, we can finally write the equation:

$$\frac{d\vec{W}}{dt} = \alpha \vec{W} - \frac{1}{\beta} \mathcal{J} (I + \xi \bar{\Omega} W)^{-1} \bar{\Omega} \bar{S}(t), \quad (\text{B4})$$

which is our final result. We note that $\bar{\Omega} = A^t (\bar{A}A^t)^{-1} \bar{A}$ is the most general description of a non-orthogonal projection operator. In the matricial limit $P \rightarrow I$, then $\bar{A} \rightarrow A$ and thus the projector becomes orthogonal again.

It is also easy to see that for $P = \pm I$, then $\bar{A} = \pm A$. As such, $\bar{\Omega}$ is indeed an invariant under this symmetry. In fact, $(\bar{A}A^t)^{-1} = \pm (AA^t)^{-1}$, and thus $\bar{\Omega}$ is invariant. However, $\bar{S} \rightarrow \pm S$, which means that this is simply a change of current flow. Although currents in a circuit are defined up to a change of direction, this implies that the circuit is not invariant under this symmetry.

Appendix C: Matrix Inverse

Let us now prove an inversion equation, where we assume that B and $\Omega + B$ are invertible:

$$(\Omega + B)^{-1} = B^{-1} + X \quad (\text{C1})$$

full rank by construction. Using the result of Eq. (C7) for the inverse $(\bar{\Omega} + B)^{-1}$ and derived in Sec. C, we can now obtain the final equation:

and aim to find the matrix X . By definition, we have:

$$\begin{aligned} I &= (B^{-1} + X)(\Omega + B) \\ &= (B^{-1}\Omega + X(\Omega + B) + BB^{-1}) \\ &= (B^{-1}\Omega + X(\Omega + B) + I). \end{aligned} \quad (\text{C2})$$

Using this identity, we can find the matrix X by inversion:

$$\begin{aligned} X &= -B^{-1}\Omega(\Omega + B)^{-1} \\ &= -B^{-1}\Omega(B^{-1} + X) \\ &= -B^{-1}\Omega B^{-1} - B^{-1}\Omega X, \end{aligned} \quad (\text{C3})$$

which can be rewritten as:

$$X = -(I + B^{-1}\Omega)^{-1} B^{-1} \Omega B^{-1}. \quad (\text{C4})$$

This implies the following inversion formula:

$$(\Omega + B)^{-1} = B^{-1} - (I + B^{-1}\Omega)^{-1} B^{-1} \Omega B^{-1}, \quad (\text{C5})$$

which is the identity we use to reach the final equation, and requires only the invertibility of the matrices B and $\Omega + B$, but not the invertibility of Ω . Such identity is important since in our case Ω represents a projector operator, meanwhile B represents $W^{-1}/(r - 1)$. Starting from the identity $I = (\Omega + B)(B^{-1} + X)$, we obtain the identity:

$$(\Omega + B)^{-1} = B^{-1} - B^{-1}\Omega B^{-1}(I + \Omega B^{-1})^{-1}, \quad (\text{C6})$$

which implies that:

$$(I + B^{-1}\Omega)^{-1} B^{-1} \Omega B^{-1} = B^{-1}\Omega B^{-1}(I + \Omega B^{-1})^{-1}. \quad (\text{C7})$$

This is the result we used in Sec. B in order to derive our main result.

Appendix D: Finite size effects

We now mention some observed factors influencing the quality of the power law. The number of memristors controls the emergence of the power law decay. Numerically, we observe that $M \approx 100$ is enough to have a faithful power law. In Fig. 4 we can see that when L/M is fixed and $M \rightarrow \infty$, the limit M can be considered as a thermodynamic limit, i.e., the power law emerges for large M .

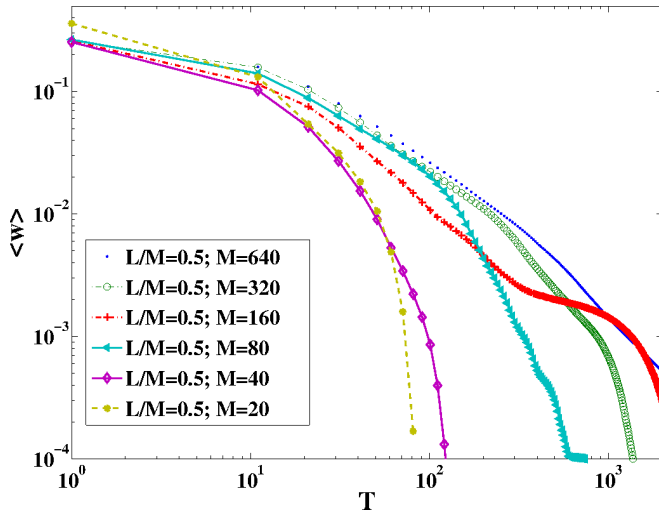


FIG. 4. Average relaxations for fixed ratios $L/M = 0.5$, with $M = 20, 40, 80, 160, 320, 640$ and initial memristors set at $w_i = 1$. These are not averaged over many quenched dynamics, but single simulations. We observe that for increasing values of M , the curves suppress the fluctuations and converge to the slow dynamics phenomenon for the average memory.